International Journal on Magnetic Particle Imaging
Vol 4, No 2, Article ID 1811004, 5 Pages

Infinite Science Publishing

Research Article

Novel Field Geometry Using Two Halbach Cylinders for FFL-MPI

Matthias Weber[a,*] · Jonas Beuke[a] · Anselm von Gladiss[a] · Ksenija Gräfe[a] · Patrick Vogel[b] · Volker C. Behr[b] · Thorsten M. Buzug[a]

[a] Institute of Medical Engineering, University of Lübeck, Lübeck, Germany
[b] Department of Experimental Physics 5 (Biophysics), University of Würzburg, Würzburg, Germany
[*] Corresponding author, email: {weber,buzug}@imt.uni-luebeck.de

Received 25 November 2016; Accepted 14 November 2018; Published online 28 November 2018

Abstract

Magnetic Particle Imaging (MPI) offers several methods for encoding magnetic materials in three-dimensions. The complexity of the imaging device in MPI using a field free line (FFL) is the biggest challenge in realizing such devices. This is especially the case for systems featuring large bores, high gradients or high temporal resolution. In this work, we suggest a novel Halbach cylinder based field generator that is able to generate an FFL with a gradient of 5 T m^{-1}. By rotating the Halbach array, FFL projections can be acquired. Furthermore, just one static drive field coil is needed for two-dimensional imaging. The presented concept could combine high gradient strength and high temporal resolution with minimum space requirements for FFL-MPI imaging in the future.

I. Introduction

Several scanner concepts have been presented in the area of FFL-MPI imaging [1–10]. Typically, either the FFL or the examined object is rotated in order to acquire projection signals. It is possible to reconstruct the acquired data with a filtered backprojection [11]. Rotating the FFL seems to be a rather straight forward method to avoid motion artifacts in animal measurements. Additionally, the rotation can be realized with much higher frequency. Unfortunately, two orthogonally aligned drive field coils are needed to shift the FFL for arbitrary angles which increases the complexity of the system [1]. Alternatively, a single drive field coil can be rotated restricting the freedom of rotation as a consequence of the cable link [3].

This work shows that the rotation of the FFL can be decoupled from the drive field. Only one static drive field coil is necessary to facilitate two-dimensional imaging. This concept is based on two opposing Halbach cylinders [12] which are discretized by permanent magnets. In the following paper, we present a system with a gradient strength of 5 T m^{-1} that is capable of acquiring high resolution three-dimensional images of a vessel-like phantom using a spiral-like trajectory. This concept has the potential to combine high gradient strength, good temporal resolution and no power consumption for generating the gradient field in an FFL-MPI system [13, 14].

II. Materials and Methods

II.I. Magnet Design

A gradient field featuring an FFL can be generated by four permanent magnets. This structure is called a quadrupole. The opposing magnets are arranged in Maxwell configuration. Both Maxwell configurations feature opposing magnetization directions [5, 15]. The corresponding magnetic fields of this structure are shown in

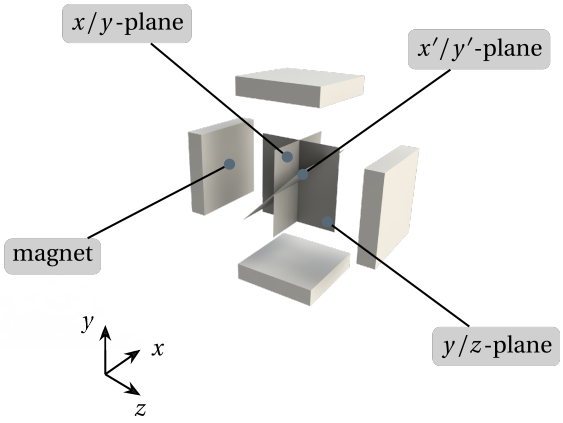

Figure 1: Schematic quadrupole. The opposing magnets are arranged in Maxwell configuration. Both Maxwell configurations feature contrary magnetization direction. The north poles of the top and bottom magnets are facing each other. The south poles of the left and right magnet are facing each other.

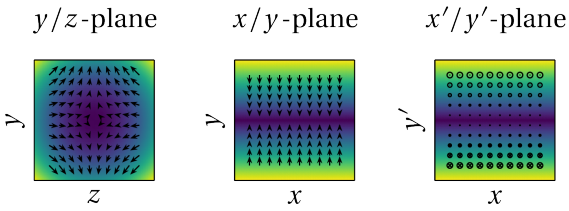

Figure 2: Magnetic fields of the quadrupole from Figure 1.

Figure 2. The field components along the x-axis cancel each other out and form an FFL. Accordingly, the x/y-plane as well as the x'/y'-plane feature a gradient field with an FFL.

The x'/y'-plane in the quadrupole setup is rotated by $\alpha = 45°$ around the x-axis. The connection between the (x, y, z)- and the (x', y', z')-coordinate system can be described as follows

$$\begin{pmatrix} x' \\ y' \\ z' \end{pmatrix} = \begin{pmatrix} \cos\alpha & 0 & \sin\alpha \\ 0 & 1 & 0 \\ -\sin\alpha & 0 & \cos\alpha \end{pmatrix} \begin{pmatrix} x \\ y \\ z \end{pmatrix}. \tag{1}$$

Thus, the magnetic fields on the x/y-plane can be described with

$$\mathbf{B}^{\gamma}_{x/y}(x, y) = \left(G\,x \sin\gamma - G\,y \cos\gamma\right) \begin{pmatrix} -\sin\gamma \\ \cos\gamma \\ 0 \end{pmatrix} \tag{2}$$

and on the x'/y'-plane with

$$\mathbf{B}^{\gamma}_{x'/y'}(x', y') = \left(G\,x' \sin\gamma - G\,y' \cos\gamma\right) \begin{pmatrix} 0 \\ 0 \\ 1 \end{pmatrix}. \tag{3}$$

These equations show that the field from (2) consists of two vectorial components and the field from (3) features only one vectorial component. Hence, only one drive field coil is necessary to shift the FFL in the x'/y'-plane for arbitrary angles.

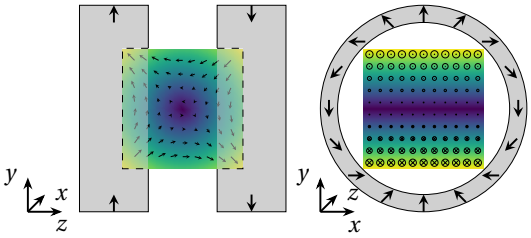

Figure 3: An FFL generated by two opposing Halbach cylinders with a gap inbetween (left as well as right). The left image shows the structure from the side. The right image shows the bore and the gradient field with the FFL.

Unfortunately, the quadrupole from Figure 1 does not feature adequate access to the x'/y'-plane and limits the bore diameter. An alternative quadrupole design can be constructed with two Halbach cylinders of the order $p = 1$ [16]. Figure 3 visualizes this assembly. Here, two Halbach cylinders, both generating a homogeneous magnetic field, are shown. By placing them next to each other and rotating one cylinder around 180°, an FFL is generated along the x-axis in the center of both cylinders. The field that is shown on the right hand side in Figure 3 corresponds to the field previously introduced in (3).

The realization of such an Halbach array was done in two steps. First, a simulation and optimization study was performed to ensure high field quality. Second, the FFL magnet was constructed on basis of the simulation results.

In the simulation study, the Halbach cylinders were discretized out of single permanent magnets. These magnets feature a size of 42 mm × 10 mm × 7.2 mm and a remanence of 1.06 T. Overall, one cylinder consists of 90 permanent magnets. The large number of magnets leads to fine discretization and therefore comes close to the performance of a continuous Halbach cylinder. The homogeneity of a gradient of 5 T m^{-1} in a circular field of view (FOV) with a diameter of 50 mm was optimized by varying the position of the single magnets. This process was based on a Gauss-Newton-Algorithm within our custom simulation environment based on the Biot–Savart law. The optimization results are visualized in Figure 4. The relative error of the simulated and ideal gradient inside the FOV is between −1.4 % and 3.8 %. The relative error between the simulated and ideal magnetic field inside the FOV is between −0.4 % to 0.9 %. It should be noted that as a result of this geometry there is no undesired magnetic field along the FFL. Thus, effects as *signal fading* or *resolution loss* can be neglected [5].

Subsequently, the FFL magnet was constructed on basis of the simulated data. To be able to precisely posi-

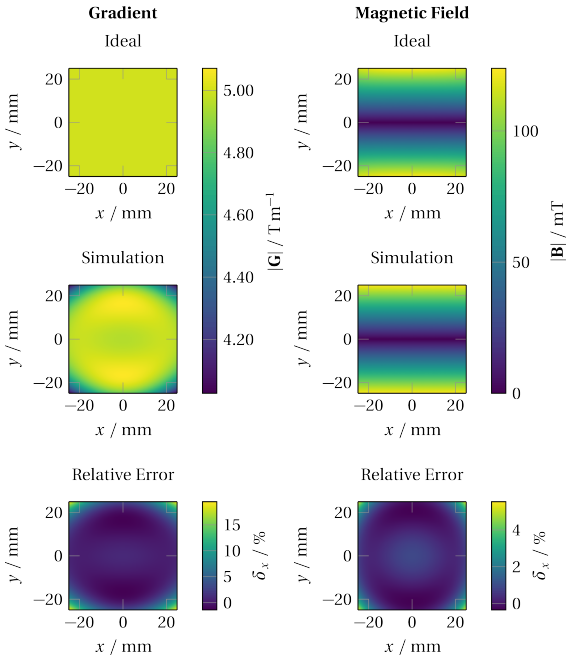

Figure 4: Optimization results of the Halbach configuration. The left column shows the ideal and simulated gradient as well as the relative error. The right column shows the ideal and simulated magnetic field and the corresponding relative error.

tion the permanent magnets, a custom template was designed with *SolidWorks* (Dassault Systèmes SolidWorks Corp., France), additively manufactured (*ProJet 3510 HD Plus*, 3D Systems, USA) and filled with the permanent magnets. The constructed template is supported by an aluminum casing. The realized FFL magnet is shown in Figure 5. For verificication, the gradient of the FFL was measured with a robot (Isel Germany AG, Germany) and a Hall probe (Model 460 3-Channel Gaussmeter, LakeShore Cryotronics, Ohio, USA).

II.II. Coil Design

Besides the FFL magnet, three solenoids were constructed and aligned inside the Halbach configuration. All are aligned along the z-axis. One solenoid generates the drive field with an amplitude of 30 mT at a frequency of 25 kHz. The drive field coil was impedance matched with a capacitive voltage divider. For generating a DC field of 30 mT the power consumption is 666 W with a current of 38.1 A. The drive field coil is surrounded by a focus field coil which is able to achieve an amplitude of 100 mT. The coils needs a DC current of 83.3 A for this amplitude, leading to a power consumption of 2.7 kW.

With large oscillating magnetic fields, peripheral nerve stimulation (PNS) and tissue heating have to be considered [17]. Therefore, a drive and focus field coil combination is a typical design approach in MPI if high gradient strength and larger FOV size are required. By

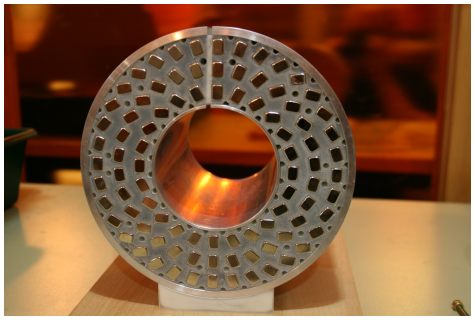

Figure 5: Realized FFL magnet.

utilizing solely a drive field coil, a field amplitude of at least 125 mT would have to be achieved (5 T m^{-1}, FOV of 50 mm diameter) resulting in enormous power requirements, voltages and current densities. Thus, by splitting up the FFL movement in a fast translation (drive field) and a slow translation (focus field, typically in the range of a few Hz), the effect of PNS and the power requirements due to eddy currents in the shielding can be reduced.

The third solenoid is surrounded by the drive field coil and was realized in a gradiometer-like configuration. It detects the generated particle signal. All coils were optimized in terms of magnetic field homogeneity and wound with enameled copper wire.

II.III. System Design

All components were subsequently integrated in a casing. The FFL magnet is positioned in a gantry that is able to rotate around the solenoids. The drive and focus field coil are aligned in a water-cooled housing. The system features a bore with a diameter of 50 mm. An overview image of the system can be seen in Figure 6. The realized system is shown in Figure 7. It does not yet contain the planned focus field coil and the water cooling.

II.IV. Phantom Imaging

For imaging experiments a vessel-like phantom was designed which features three tubes with a diameter of 1 mm each (see Figure 8). The vessel-like structure has a width of 50 mm and a height of 10 mm.

Preliminary imaging was performed by moving the phantom in a spiral-like trajectory through the FOV to emulate the rotation of the gantry. The pitch of the spiral was 1 mm per full rotation and was performed in 1 s. The phantom was filled with diluted (ratio 1:4) Resovist. Here, only the drive field coil was used to move the FFL. The acquired data of a full rotation was reconstructed using the x-space method, an inverse Radon transformation and a deconvolution using a Wiener filter [1, 11].

10.18416/ijmpi.2018.1811004

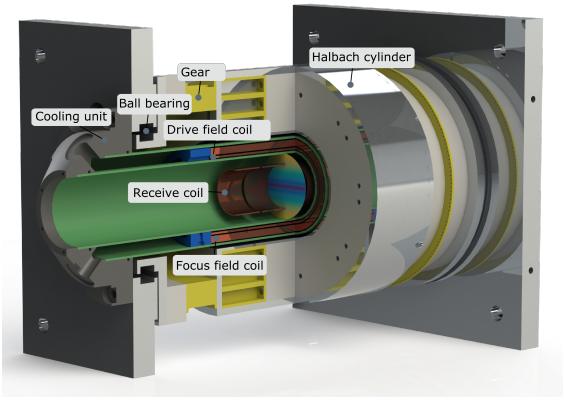

Figure 6: CAD model of the system design including the three coils as well as the mechanical components.

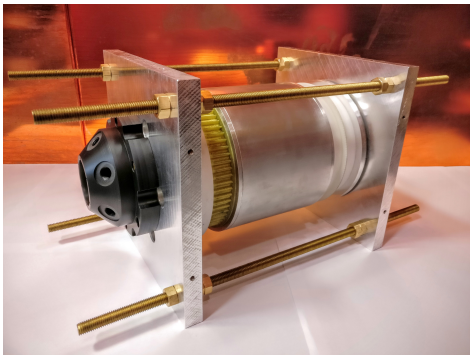

Figure 7: Realized FFL scanner.

III. Results

The field measurement verified the gradient strength of 5 T m^{-1} from the simulation. In Figure 8 an overlay image of the realized vessel-like phantom with one of the reconstructed images can be seen. Figure 9 shows the reconstructed volume. The single structures can be clearly discerned. At the bottom of the volume, parts of the tubes do not contain any tracer material. It can be seen at the top that the FFL did not move completely over the whole phantom. A FOV of 43 mm × 10 mm × 10 mm could be realized. From the dimensions of the vessel-like phantom it can be concluded that the resolution is below 2 mm.

IV. Conclusion

A new FFL-MPI concept has been presented in this paper. The first prototype with a gradient of 5 T m^{-1} was constructed. Furthermore, preliminary three-dimensional imaging of a vessel-like phantom could be performed. In the future, we are going to integrate the focus field coil in the system. Hence, it would be possible to cover a FOV with a diameter of 50 mm. Furthermore, the rotation of the gantry will allow for fast two-dimensional imaging of up to 10 frames per second. Additionally, different options for shielding the system, for instance with a copper tube around the drive and receive coil, will be evaluated.

Figure 8: Realized vessel-like phantom including an overlay of one the reconstructed images from Figure 9.

Acknowledgments

This work was supported by the LUMEN Research Group through the Federal Ministry of Education and Research (BMBF) under Grant FKZ 13EZ1140A/B as well as the German Research Foundation (DFG) under Grant BU 1436/10-1 and BU 1436/9-1. LUMEN is a Joint Research Project of the Lübeck University of Applied Sciences, Lübeck, Germany, and the Universität zu Lübeck, Lübeck, and represents its own branch of the Graduate School for Computing in Medicine and Life Sciences, Universität zu Lübeck.

References

[1] K. Bente, M. Weber, M. Graeser, T. F. Sattel, M. Erbe, and T. M. Buzug. Electronic Field Free Line Rotation and Relaxation Deconvolution in Magnetic Particle Imaging. *IEEE Transactions on Medical Imaging*, 34(2):644–651, 2015, doi:10.1109/TMI.2014.2364891.

[2] J. J. Konkle, P. W. Goodwill, O. M. Carrasco-Zevallos, and S. M. Conolly. Projection Reconstruction Magnetic Particle Imaging. *IEEE Transactions on Medical Imaging*, 32(2):338–347, 2013, doi:10.1109/TMI.2012.2227121.

[3] M. Weber, K. Bente, S. Bruns, A. von Gladiss, M. Graeser, and T. M. Buzug, A 1.4T/m Field Free Line Magnetic Particle Imaging Device, in *International Workshop on Magnetic Particle Imaging*, 142, 2016.

[4] K. Murase, S. Hiratsuka, R. Song, and Y. Takeuchi. Development of a system for magnetic particle imaging using neodymium magnets and gradiometer. *Japanese Journal of Applied Physics*, 53(6):067001, 2014, doi:10.7567/JJAP.53.067001.

[5] P. W. Goodwill, J. J. Konkle, B. Zheng, E. U. Saritas, and S. T. Conolly. Projection X-Space Magnetic Particle Imaging. *IEEE Transactions on Medical Imaging*, 31(5):1076–1085, 2012, doi:10.1109/TMI.2012.2185247.

[6] T. Knopp, T. F. Sattel, S. Biederer, and T. M. Buzug. Field-free line formation in a magnetic field. *Journal of Physics A: Mathematical and Theoretical*, 43(1):012002, 2010, doi:10.1088/1751-8113/43/1/012002.

[7] J. Weizenecker, B. Gleich, and J. Borgert. Magnetic particle imaging using a field free line. *Journal of Physics D: Applied Physics*, 41(10):105009, 2008, doi:10.1088/0022-3727/41/10/105009.

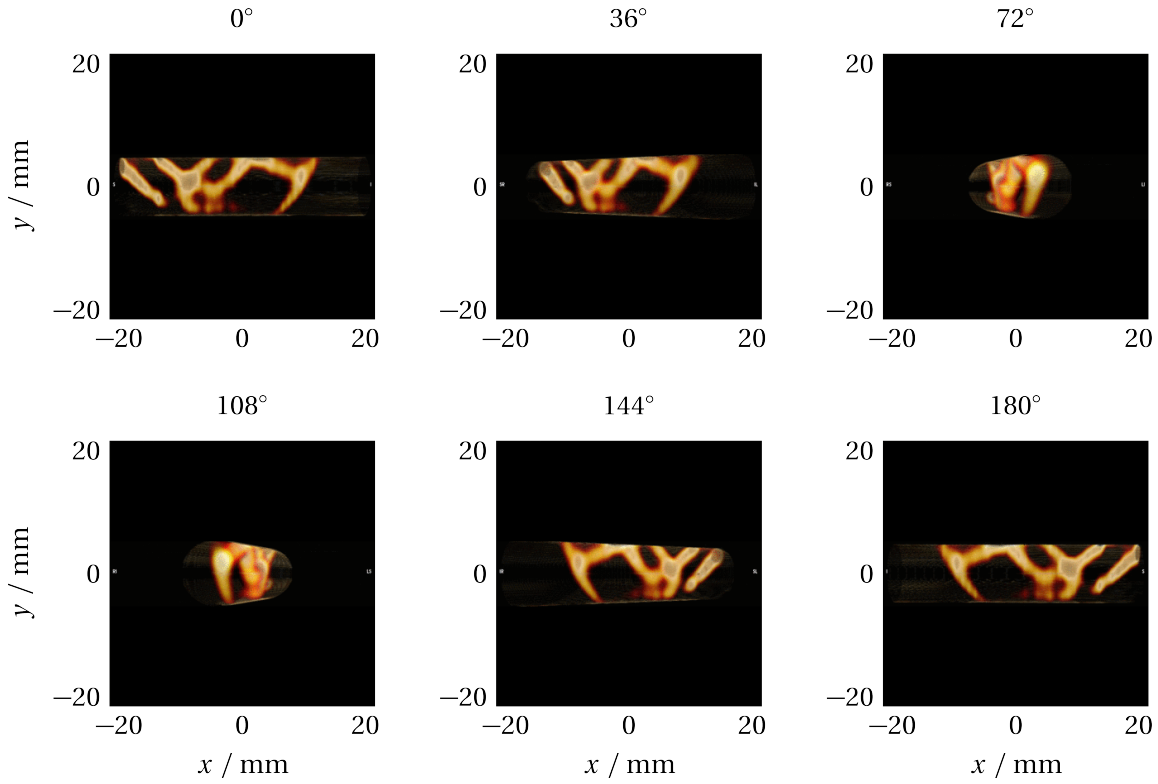

Figure 9: Three-dimensional reconstruction of the vessel-like structure. The maximum intensity projection is shown from different angulations.

[8] V. Vogel, M. A. Rückert, and V. C. Behr, MPI Cube – Fully 3D Field Free Line Scanner, in *International Workshop on Magnetic Particle Imaging*, 26, 2016.

[9] A. Tonyushkin. Single-sided hybrid selection coils for field-free line magnetic particle imaging. *International Journal on Magnetic Particle Imaging*, 3(1), 2017, doi:10.18416/IJMPI.2017.1703009.

[10] G. Rudd and A. Tonyushkin. Permanent Magnet Selection Coils Design for Single-Sided Field-Free Line Magnetic Particle Imaging. *International Journal on Magnetic Particle Imaging*, 4(1), 2018, doi:10.18416/IJMPI.2018.1809001.

[11] T. Knopp, M. Erbe, T. F. Sattel, S. Biederer, and T. M. Buzug. A Fourier slice theorem for magnetic particle imaging using a field-free line. *Inverse Problems*, 27(9):095004, 2011, doi:10.1088/0266-5611/27/9/095004.

[12] K. Halbach. Design of permanent multipole magnets with oriented rare earth cobalt material. *Nuclear Instruments and Methods*, 169(1):1–10, 1980, doi:10.1016/0029-554X(80)90094-4.

[13] M. Weber, Magnetic Particle Imaging, Neuartige Bildgebungskonzepte mit einer feldfreien Linie. Lübeck: Infinite Science Publishing, 2017, ISBN: 978-3-945954-42-3.

[14] M. Weber and T. M. Buzug, Magnetic field-generating device for magnetic particle imaging, WO/2017/050789, 2017.

[15] T. Knopp, M. Erbe, T. F. Sattel, S. Biederer, and T. M. Buzug. Generation of a static magnetic field-free line using two Maxwell coil pairs. *Applied Physics Letters*, 97(9):092505, 2010, doi:10.1063/1.3486118.

[16] H. Raich and P. Blümler. Design and construction of a dipolar Halbach array with a homogeneous field from identical bar magnets: NMR Mandhalas. *Concepts in Magnetic Resonance Part B: Magnetic Resonance Engineering*, 23B(1):16–25, 2004, doi:10.1002/cmr.b.20018.

[17] P. W. Goodwill and S. M. Conolly. The X-Space Formulation of the Magnetic Particle Imaging Process: 1-D Signal, Resolution, Bandwidth, SNR, SAR, and Magnetostimulation. *IEEE Transactions on Medical Imaging*, 29(11):1851–1859, 2010, doi:10.1109/TMI.2010.2052284.